VEHICLE CABIN ROOF THERMAL SHIELD USING PHASE CHANGE MATERIAL

CHỐNG NÓNG MÁI XE ÔTÔ SỬ DỤNG VẬT LIỆU CHUYỂN PHA

Nguyen Vu Lan
Ho Chi Minh City University of Technology and Education

Received 15/12/2015, Peer reviewed 04/01/2016, Accepted for publication 11/01/2016.

ABSTRACT

This paper presents amelioration for vehicle roofing design to improve its total thermal resistance. The key concept is to utilize phase change material properties to trap the heat from solar radiation and then release it back to the environment by means of the naturally favored external convection when the vehicle is running or during the nocturnal cycle. Experimental and numerical analyses have been conducted to compare the thermal performance of the new design and the normal roofing with different colors. A general mathematic equation system has also been derived for the thermal process through of the roof. Results show that the new design could effectively reduce the downward heat flow from the roof into the cabin. As a consequence, the cooling load of the cabin is significantly lower.

Keywords: *Cool roof, solar roof, vehicle roof*

TÓM TẮT

Bài báo này giới thiệu một giải pháp thiết kế mới cho mái xe ôtô nhằm cải thiện nhiệt trở của lớp mái xe. Điểm đặc biệt *chính của thiết kế là việc tận dụng những đặc tính của vật liệu chuyển pha để thu toàn bộ nhiệt lượng từ bức xạ mặt trời lên mái sau đó giải phóng ngược nhiệt lượng này ra môi trường thông qua cơ chế truyền nhiệt đối lưu cưỡng bức xảy ra khi xe chạy hoặc vào khoảng thời gian tắt nắng về* đêm. Các nghiên cứu *thực nghiệm và mô phỏng đều được thực hiện để so sánh tính năng của thiết kế mới so với cấu trúc mái thông thường của các xe ôtô với những* màu sơn khác nhau. *Tác giả đã thiết lập một hệ phương trình toán học tổng quát* mô tả quá trình trao đổi nhiệt *ứng với thiết kế này. Kết quả cho thấy thiết kế mới giúp giảm thiểu rất hiệu quả dòng nhiệt xuyên qua mái vào trong xe. Do đó, nhiên liệu tiêu thụ cho việc điều hòa nhiệt độ xe cũng sẽ được giảm thiểu đáng kể.*

Từ khóa: *Kiểu mái mát, Mái năng lượng mặt trời, Mái xe ôtô*

1. INTRODUCTION

A vehicle roof, like a metal sheet roof of a house, may receive a incident solar radiation up to more than 1000W/m^2 in clear sky conditions and from 20% to 95% of this radiation may be absorbed [1]. In recent years, many approaches of designing roofing structure have been obtained in order to utilize the incident solar irradiation on the roof area and/or to reduce downward heat flow from roof into cabin space. The main methods can be classified into 2 groups. The first group bases on the concept of minimizing solar radiation absorption of the roof layer, such as attaching solar collectors and photovoltaic systems to cover the roof surface area. In this way, the incident infrared radiation is not only prevented from reaching the roof, but also collected to produce electricity to supply to vehicle [2~5]. Meanwhile the second group uses modification of thermal properties of the roofing layer. Light painting colors of the roof can obviously reflect more and absorb less solar radiation. Unfortunately, the painting color of a car affects much on its beauty and price. For many vehicle designs, black color is more impressive than others. Addition of more insulation materials into the roof could help to increase thermal resistance of the roof [6]. Usually, air

conditioner is used to cool down the cabin while heat from the roof is still flowing downward. Obviously, if thermal resistance of the roof is improved, less energy will be consumed for the cooling purpose. Normal roofing structure of modern vehicles is illustrated as in Fig. 1.

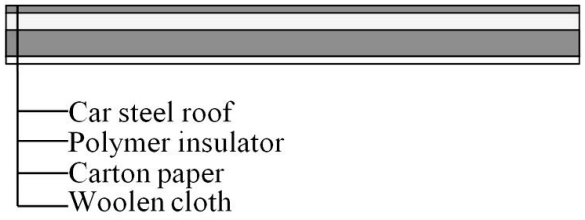

Fig 1. *Layer structure of normal vehicle*

Phase change materials (PCMs) were first used for thermal storage in 1980 [7]. The special ability of changing phase and absorbing/releasing heat of PCMs makes them become very useful in attempts of maintaining constant temperature condition or shifting the peak time of thermal load in a space [8]. In this paper, the new design was developed from the normal roof structure of vehicles available in modern markets. A phase change material has been inserted in between insulator layer(s) and the upper metal sheet layer. It is expected to show that phase change properties of PCM may not only be utilized to store thermal energy as in heat storage applications [9~11] but also to improve thermal insulation effect of the PCM combined roofing structure. Fig. 2 illustrates the design. The vehicle roofing material is the standard and real roof of Toyota sedan cars in the market. Four different colors including black, grey, yellow and white have been tested. Each sample having a dimension of 0.6m × 0.6m is placed horizontally under a simulated solar radiation using high power electrical lights. In order to enable new product development with as little cost as possible without the need of building up other prototype models, this paper has also built up mathematic equations to be used in further analysis of the design. As a result, with related data assumption, a suitable amount of PCM for the roof to obtain an expected room temperature and an appropriate PCM distribution inside the roof may be found. The precision of the simulation models has also been tested by experimental data to prove that they may be used to develop designing and manufacturing of advanced vehicle roof.

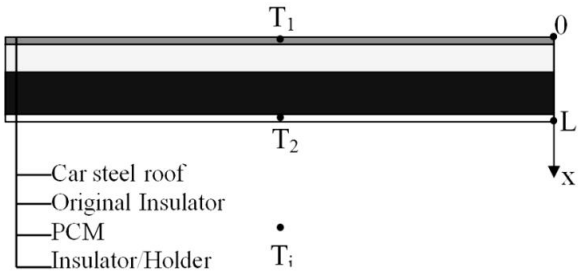

Fig 2. *Novel design structure of the vehicle roof*

2. EXPERIMENT SETUP

The experimental system consists of different models of car roof acting as the roof of a small–scale isolated room, temperature data acquisition system using thermal couples and a solar radiation simulating system. A solar simulation system is constructed to supply a constant radiation power incident on to the roofing surface. It includes 4 halogen lamps of electric power of 500W/110V. In order to gain a consistent assumption of the solar radiation on the roofing surface, the lights are fixed at constant distance and with the same supplied power so that the average incident radiation is kept equal to 950W/m^2 when they are all turned on. Besides, temperature of the ambient air surrounding the whole experimental system is always kept to be around 25^{o}C. The small–scale insulated room, which has dimensions of 600mm × 600mm × 600mm, is constructed by using 60mm thick porous thermal insulator plates to cover at the bottom and 4 lateral sides of the room which make sure that heat loss from the air inside the room to outside ambient air is negligible. The top side is covered by one of the models of the roofing in each experiment.

In order to make sure that under the same experimental condition the new model

has a better thermal resistance than other models which are available in market, the models of each color (black, grey, yellow and white) used for testing include: a normal model (#1) which is the normal car roof; and a new model (#2) inside which a layer of PCM39D (2kg) is inserted (Fig. 2). Table 1 shows the thermal parameters of materials used to make experiment models. Absorptivity values of black, grey, yellow and white painting colors are 0.95; 0.85; 0.55 and 0.40, repectively.

T-type thermocouples with error of ±0.2°C are used to measure surface temperatures of the upper and lower metal sheet layers, of surfaces of PCM layer, of insulation layer and of the ambient air. The thermocouples are connected to an ADAM recorder which is in turn connected to the computer via RS232 serial connection. A typical arrangement of thermal couples in the experiment of model (#2), which consists of PCM, is shown in Fig. 2.

Table 1. *Material parameters used in the experiment models*

Material	Density (kg/m^3)	Thermal conductivity (W/(mK))	Specific heat (kJ/(kg.K))	Melting temp. (°C)	Thickness (mm)
1. PCM39D	800	(---)[a]	(---)[a]	» 39	10
2. Car roof	7861.2[12]	51.92[12]	0.51[12]	-	1
3. Normal insulator	40	0.015	0.8	-	7
4. Air	1.0	0.026[13]	1.0	-	540

[a] Refer to Eq. (9) and Eq. (10)

3. MATHEMATIC FORMULATION

Convection and radiation from upper roof surface to the surrounding ambient air are considered in thermal response analyses of roof models with/without PCM. Heat conduction solution is obtained for the solid layers, liquid/solid PCM and for air space inside the insulated room (since the heat flux is transferred downward, which impedes convection effect). The solid layers are assumed to have constant thermal parameters (except the PCM layer) and to be in good thermal contact, which means that the interface resistance is zero. Due to the very small thickness of the metal layers (0.3mm), PCM layer (in case PCM models are tested) (7mm) and insulator layer (5mm), heat loss on the horizontal direction is negligible. Thus, a 1D heat transfer model can be employed here. Accordingly, equations (1) to (2) are used to form the mathematic model of the heat transfer process in the roofing without any internal heat source. The outer surface of the roofing model is subjected to the simulated solar radiation Q_{solar}, external convection and surface to ambient radiation q_{rad}. Eq. (1) is the governing partial differential equation (PDE) at this surface. For the solid layers and the insulator(s), only heat conduction is considered as shown in Eq. (2).

$$-k_{metal}\left.\frac{\partial T_1}{\partial x}\right|_{x=0} = \alpha Q_{solar} - q_{rad} - h_{ex}(T_1 - T_a) \quad (1)$$

$$\rho_i C_i \frac{\partial T_i(x,\tau)}{d\tau} = k_i \frac{\partial^2 T_i(x,\tau)}{\partial x^2} \quad (2)$$

Where in, a is absorptivity, x and t are the space and time coordinates, respectively; the index *i* indicates the ith layer; T_i is the temperature of the ith layer; ρ_i, C_i, k_i and k_{metal} are the density, the specific heat and the thermal conductivity of the ith layer material or metal layer, respectively.

Although transient value of convective heat transfer coefficient of roofing surface can be calculated more precisely during the nu-

merical simulation process, it is necessary to estimate its approximated average value and thus the external convection rate of the roof during experiments can be evaluated. When no external wind exists, according to G.N. Tiwari [14], a roughly approximated value of the external convective heat transfer coefficient for the external facing–upward horizontal roof surface is determined from Eq. (3) and (4). With the characteristic dimension $X = (L_o + B_o)/2 = 0.6$m, this gives an average h_{cx} of 6.7351 W/m^{2}K in a temperature range of 25–95^{o}C with an average ambient temperature of 25^{o}C.

$$Gr \times Pr = \frac{g\beta\rho^2 X^3 \Delta T}{\mu_d^2} \times Pr \quad (3)$$

$$h_{ex1} = 0.14 \times \frac{K}{X} \times (Gr\,Pr)^{1/3} \quad (4)$$

When external wind occurs, the empirical values in W/m^{2}K of the external convective coefficient can be derived from the method of Ito et al. [15] as in Eq. (5).

$$h_{ex2} = \begin{cases} 8.053 \times v^{0.605} & \text{if} \quad v > 2(m/s) \\ 12.249 \times v^{0.605} & \text{if} \quad v < 2(m/s) \end{cases} \quad (5)$$

Wherein v is the external wind speed (m/s).

The radiation rate (q_{rad}) is given by Eq. (6) and radiation heat transfer coefficient is given by Eq. (7).

$$q_{rad} = \varepsilon\sigma\left(T_1^4 - T_{sky}^4\right) \quad (6)$$

$$h_{rad} = \varepsilon\sigma\left(T_{sky}^2 + T_1^2\right)\left(T_{sky} + T_1\right) \quad (7)$$

Wherein e is the surface emissivity, s is the Stefan–Boltzmann constant, and T_{sky} is the sky temperature which is approximately equal to (T_a – 12) [16].

The melting and solidifying processes of PCM are treated in terms of the variation of the specific heat value of the PCM in which the change of latent heat capacity is already included. Here the effective heat capacity model is used [17]. Heat transfer equation in the PCM layer is shown as Eq. (8), in which equivalent thermal conductivity k_{PCM} and effective specific heat Cp_{PCM} of PCM are functions of nodal temperature. Eq. (9) shows the function of k_{PCM} [W/(m.K)] basing on the thermal conductivity of PCM in solid state and liquid state, respectively. Cp_{PCM} [kJ/(kg.K)] can be approximately modified into a stepwise form as in Eq. (10). It is important to notice that the following assumptions have been used: (i) density of the PCM is constant in both phases, (ii) there is no volume change during the phase transitions and (iii) thermal conductivity and effective specific heat are constant in the solid phase and liquid phase. The insignificant convection effect inside the thin layer of liquid PCM in the roofing is neglected due to its small (less than 1cm) thickness and is represented by the equivalent thermal conductivity at liquid phase k_L.

$$\rho_{PCM} Cp_{PCM} \frac{\partial T(x,\tau)}{d\tau} = k_{PCM} \frac{\partial^2 T(x,\tau)}{\partial x^2} \quad (8)$$

$$k_{PCM} = \begin{cases} k_{S-PCM} & T < T_{melt\text{-}min} \\ k_{S-PCM} + \dfrac{k_{L-PCM} - k_{S-PCM}}{T_{melt\text{-}max} - T_{melt\,min}} (T - T_{melt-min}) & T_{melt\text{-}min} \le T \le T_{melt\text{-}max} \\ k_{L-PCM} & T_{melt\text{-}max} < T \end{cases} \quad (9)$$

$$Cp_{PCM} = \begin{cases} Cp_{S\text{-}PCM} & T < T_{melt\text{-}min} \\ \dfrac{H}{(T_{melt\text{-}max} - T_{melt\text{-}min})} + \dfrac{Cp_{S-PCM} + Cp_{L-PCM}}{2} & T_{melt\text{-}min} \le T \le T_{melt\text{-}max} \\ Cp_{S\text{-}PCM} & T_{melt\text{-}max} < T \end{cases} \quad (10)$$

For the used PCM, thermal conductivity and effective specific heat values are:

$$k_{PCM} = \begin{cases} 0.17 & T < 311.45K \\ 0.21 & 311.45K \le T \le 313.45K \\ 0.25 & 313.45K < T \end{cases} \quad (9a)$$

$$Cp_{PCM} = \begin{cases} 1.7 & T < 311.45K \\ 458 & 311.45K \le T \le 313.45K \\ 1.9 & T > 313.45K \end{cases} \quad (10a)$$

Because the proposed PCM–based roofing simulation is a transient process, initial and boundary conditions must be set appropriately before the calculation starts. With reference to the coordinate origin indicated in Fig. 4, initial conditions are: initial temperature of all layers is 298.15K and $Q_{solar}(t=0) = 950W/m^2$. The simulation is conducted during time period $t \pounds t_{max}$ (s).

When the incident solar radiation occurs on the roof surface, T_1 is higher than the melting temperature T_m of the PCM inside the roofing ($T_1 > T_m$) as well as the ambient temperature ($T_1 > T_a$), heat can be transferred from the top surface downward through the PCM layer to the bottom surface. This results in melting of the PCM. When there is no solar radiation on the roof surface, the top surface will be cooled down fastest and heat from inside air and the PCM will be released upward from the top. For models of roofing without PCM, equations from (1) to (7) are applied, while for models of roofing with PCM, equations from (1) to (10) are applied. Simulation has been executed by COMSOL Multiphysics software with changeable time step size to investigate the system. Convergence has also been checked at each time step with the convergence criterion of 10^{-3}. It is noted that since the experiments were done with indoor condition (wherein the ambient temperature was constant at 25°C), the value of T_{sky} in Eq. (7) was thus set at 25°C.

Considering that the inside air of the insulated room is adiabatic with outside ambience during the whole experiment process, the amount of heat gets into the isolated room through its roof model can be represented by the indoor temperature. Obviously, for the same desired indoor temperature 25°C, required energy for air conditioning inside the room will be reduced if the difference between the instant room temperature and the desired value is less. Eq. (11) and Eq. (12) show the energy saving rate x(%) of heat coming into the room when using normal model (E_{normal}) and the new model (E_{PCM}).

$$\frac{E_{PCM}}{E_{normal}} = \frac{\int_{t=0}^{t_{stop}} m_{air}.C_{pair}.(T_{i-PCM} - T_{i-desired})dt}{\int_{t=0}^{t_{stop}} m_{air}.C_{pair}.(T_{i-normal} - T_{i-desired})dt}$$

$$= \frac{\sum_{k} (T_{i-PCM-k} - T_{i-desired})\Delta t}{\sum_{j} (T_{i-normal-j} - T_{i-desired})\Delta t} \quad (11)$$

$$\xi(\%) = 1 - \frac{E_{PCM}}{E_{normal}} \quad (12)$$

Wherein, $T_{i-desired}$ is the desired temperature to be maintained inside the cabin; $T_{i-PCM-k}$ is the temperature of the isolated–room air when using PCM roof and $T_{i-normal-j}$ is the temperature of the isolated–room air when using normal roof at each step of data acquisition Δt.

4. RESULTS AND DISCUSSION

4.1. Experimental results and analysis

Eight–hour measurements were recorded to analyze the roof models in this paper. The experimental data file contains: (a) time period since start up in seconds, each period was 20s and (b) the instantaneous temperature on all channels at the end of each period. Fig. 5 shows plots of temperature variation comparison over time for the yellow models with and without PCM at top surface, bottom surface and indoor air, respectively no external wind was allowed. The effect of external wind (5.5m/s) on the thermal performance of the yellow models is shown in Fig. 6. In each of these plots, T_a indicates the ambient temperature of the surrounding air; T_1 indicates the temperature of the uppermost surface of

the roofing; T_2 indicates the temperature of the lowermost surface of the roofing and T_i indicates the average air temperature inside the isolated room; the term "normal" indicates the normal model without PCM and the term "PCM" indicates the new design. In all experiments, surrounding air temperature was kept constantly at 25°C; lights were turned on to heat up the models for 4 hours and successively turned off for the next 4 hours for cooling period.

It was not surprised to see that the measured temperature values in these experiments were all higher than their actual values in the real outdoor weather condition. It was because the experiments were conducted indoor without external wind and under a simulated 1000W/m^2 solar radiation, which is equivalent to solar radiation of a very clear sky day. As a result, only a small part of the absorbed heat on the roof was released back to outside ambiance due to natural convection and radiation, while its main part was transferred into the cabin through the roof. This was also the harshest weather condition in which heat transfer rate through the roof into a cabin would be the most. Obviously, if a roof design could work well in such condition, it would be an excellent solution in the normal weather condition which was less stifling. Besides, this experimental condition could help to reduce unexpected interfering parameters and thus thermal response comparison among models would be more precise. Moreover, further predictions for the new design in varied conditions could be obtained from numerical analyses.

It can be seen from the experiment data (Fig. 3) that the temperature value at measured points were higher in the normal roof model than in the PCM model. It revealed that the addition of the PCM layer truly increased the total thermal resistance of the roof. Furthermore, this thermal resistance increment was not a constant value but a nonlinear one due to the phase change process of the PCM. During the melting process of the PCM, the heat flow was absorbed completely and only a small heat flow got into the room under the limit of the melting temperature of the PCM. This fact also suggested the use of PCM having melting temperature closer to the desired room temperature (e.g. 25°C) in order to lower down the heat flow rate getting into the room during the melting process. However, choosing lower melting temperature PCM would lead to a shorter melting process as the PCM layer would receive bigger heat flow which was proportional to the temperature difference between the roof surface and the PCM layer. This conclusion was also approved by the simulation results in section 4.2.1.

It was also found that the melting period of PCM lasted longest for the case of white color model and shortest for the case of black color model. It was obviously because the absorptivity of the black model was the highest and that of the white model was the lowest out of the 4 model colors (Table 2), thus a bigger downward heat flow was obtained in the black model than in the white model. When the melting process ended, PCM layer could not trap the downward heat flow significantly. And the inside room air temperature increased with almost the same rate as in case of the normal roof. This was a very important notice for designing the PCM roof in such a way that the amount of PCM should be chosen properly so that it could be enough to maintain the melting process as long as possible (e.g. during the time that the car is parked under the sun). This time period was assumed here to be 4 hours.

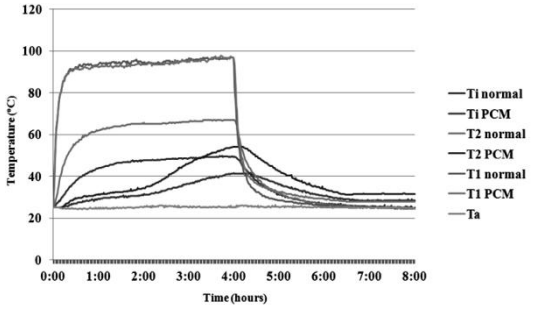

Figure 3. *Temperature responses of yellow roof models with/without PCM (no external wind)*

The melting period of PCM was prolonged significantly when external wind blew over the roof surface (Fig. 4) at the rate of 5m/s. (This condition may happen with normal breezing or when the car runs at rather low speed.) It was because convective heat loss would increase much more than that in the experiment condition without external wind. Consequently, the downward heat flow was much less too. Thus heat absorption ability of the same amount of PCM increased. This was revealed from the value of the indoor air temperature in Fig. 4. Such result may give another suggestion about the designed amount of PCM basing on the weather condition at a specific area. Less PCM could be used when more external wind was available.

Although PCM did help to reduce heat flow into the cabin during the heat period, the heat amount it absorbed may also transfer into the cabin even when there was no incident solar radiation on the roof. This could be seen from the cooling period in both Fig. 3 and Fig. 4. Fortunately, since the top side of the roof cooled down fast when the solar radiation was off, the stored heat inside PCM could also be released upward back to the ambiance. Cooling effect in this direction would be favored more thanks to the forced convection made by external wind (if available) (Fig. 4). For this reason, the total heat entering the cabin during the whole 8-hour period through the PCM roof was much less than that through the normal roof. Experiment results of all models with four colors are summarized in Table 2. The temperature values in this table were derived after 4 hours of heating. The energy saving ratio was quite high for all of the models. This proved that the new roof design would really help to reduce significantly the fuel consumption for cabin air conditioning purpose.

4.2. Numerical results and analysis

Basing on equations and values derived in Section 2, simulating models have been established by COMSOL Multiphysics software.

In order to estimate effect of the melting temperature of PCM on the thermal performance of the new design, three different melting temperature values were assumed for the used PCM, which were 30°C, 39°C and 50°C, respectively. The simulations were computed with the assumption of no external wind and all other thermal parameters were kept the same. Results (Table 3) showed that the lower the melting temperature, the shorter the melting process. The period in which the isolated-room air received heat was longer, thus it reached to a higher maximum value. However, the energy saving ratio was higher for the lower melting temperature.

Table 4 shows the effect of latent heat capacity of the installed PCM. It is clear that the higher the value of the latent heat capacity of the PCM is, the more heat can be trapped and the longer the melting period is. As a result, the designed weight of PCM in the new roof model to maintain the same melting period in the same weather condition would vary according to the latent heat capacity. Besides, the energy saving ratio was also higher in case of the higher latent capacity of PCM. To compare, all simulations here were conducted with the assumption of no external wind and all other thermal parameters were kept the same with PCM 39D.

As the ambient temperature increased, heat loss from the roof to surrounding ambiance was less. Accordingly, the downward heat flow into the room became stronger. Besides, when the ambient temperature was higher than the melting temperture of PCM, it was also surrounding air to contribute heat into the cabin during the cooling period. In this case, the stored heat in PCM would not be able to be released back to outside air. For this reason, the melting temperature of PCM should be chosen depending on the weather condition where the design would be applied. The simulations here were computed with PCM 39D without external wind and all other thermal parameters were kept the same. Table 5 shows the variation of energy saving ratio according to the variation of ambient temperature.

External wind contributed excellently to the thermal performance of the new design (Table 6). It was because with the help of external wind, forced convection took place

more strongly on the surface of the roof. This resulted in much lower downward heat flow during heating period and much higher upward heat loss from the roof to the ambient air during the cooling process. Accordingly, the space inside the cabin did receive less heat in the whole heating – cooling cycle, thus the energy saving ratio was quite high. The simulations here were computed with PCM 39D with different external wind velocities while all other thermal parameters were kept the same.

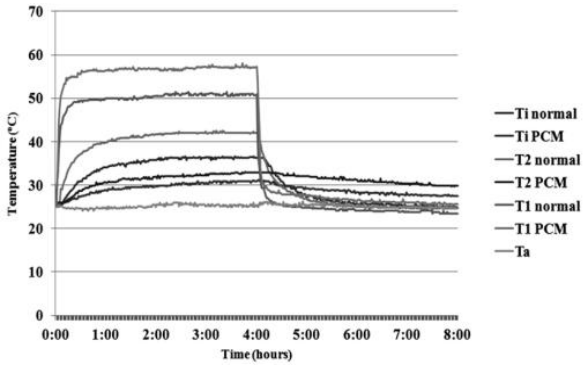

Figure 4. *Temperature responses of yellow roof model with/without PCM (with external wind)*

Table 2. *Experiment result comparison*

Color	External wind	With PCM	T_1 (°C)	T_2 (°C)	T_i (°C)	x(%)
Black	No	Yes	113.5	65.2	49.2	25.24
Black	No	No	113.2	79.1	56.3	
Grey	Yes	Yes	57.1	32.9	30.8	40.06
Grey	Yes	No	56.9	45.9	37.9	
Grey	No	Yes	108.7	60.6	44.5	40.04
Grey	No	No	106.2	74.9	54	
Yellow	Yes	Yes	57.3	32.9	30.8	39.31
Yellow	Yes	No	51.1	42.1	36.2	
Yellow	No	Yes	96.7	54	41.4	30.71
Yellow	No	No	96.4	66.5	49.1	
White	No	Yes	92.1	52.5	40.1	38.90
White	No	No	90	63.9	47.4	

Table 3. *Effect of melting temperature of pcm*

Color	External wind	With PCM	PCM melting temperature (°C)	Melting period (min)	x(%)
Grey	No	Yes	30	31	46.56
Grey	No	Yes	39*	40	40.03
Grey	No	Yes	50	47	32.04
(* experimental condition)					

Table 4. *Effect of latent heat capacity of pcm*

Color	External wind	With PCM	Latent heat (kJ/kg)	Melting period (min)	x(%)
Grey	No	Yes	60	23	21.13
Grey	No	Yes	88*	40	40.03
Grey	No	Yes	120	66	62.04
(* experimental condition)					

Table 5. *Effect of ambient temperature*

Color	External wind	With PCM	Ambient temperature (°C)	x(%)
Grey	No	Yes	25*	40.03
Grey	No	Yes	35	38.13
Grey	No	Yes	45	32.04

(* experimental condition)

Table 6. *Effect of external wind speed*

Color	External wind	With PCM	Wind speed (m/s)	Wind speed (km/h)	x(%)
Grey	Yes	Yes	5*	18	40.06
Grey	Yes	Yes	10	36	70.71
Grey	Yes	Yes	15	54	88.90

(* experimental condition)

5. CONCLUSION

In this paper, a new design of roofing for vehicles was made by inserting a layer of PCM to the roof structure in order to reduce the heat transferred through the roof into the cabin space. Both experimental and numerical results have shown that the new design has a better thermal performance than the normal roof structure of available vehicles in the market. In the above-mentioned experiment condition, the new design may help to reduce up to about 40% of the energy amount required for cooling down the heat entering into the cabin from the roof. In case external wind is present due to natural wind or movement of the car in use, even higher saving rate could be achieved. The paper also suggests the trends and conditions for choosing the most suitable PCM type and amount in real design according to the weather condition such as ambient temperature, melting temperature and latent heat capacity. This is a promising design which could be massively produced due to its simple structure and reasonable price.

ACKNOWLEDGEMENTS

The authors would like to send the sincerest thanks to the Mechanical Engineering Department of Kun Shan University, Tainan, Taiwan and Ho Chi Minh City University of Technology and Education for all their supports during the research.

REFERENCES

[1] H. Suehrcke, E.L. Peterson and N. Selby, *Effect of roof solar reflectance on the building heat gain in a hot climate*. Energy and Buildings 40, 2224–2235 (2008).

[2] Information on http://www.solarelectricalvehicles.com/

[3] Information on http://en.wikipedia.org/wiki/Solar_vehicle

[4] Information on http://www.thinksolarenergy.net/121/solar-power-in-cars/solar-energy-solar- systemc

[5] Han, J, L Lu and H Yang, *Thermal behavior of a novel type see-through glazing system with integrated PV cells, Building and Environment*, Vol.44, No.10, pp.2129-2136 (2009).

[6] Yaping Cui, Jingchao Xie, Jiaping Liu, Song Pan, *Review of Phase Change Materials Integrated in Building Walls for Energy Saving*, Procedia Engineering 121, 763 – 770 (2015).

[7] A. Sharma, V.V. Tyagi, C.R. Chen, and D. Buddhi, *Review on Thermal Energy Storage with Phase Change Materials and Applications*, Renewable and Sustainable Energy Reviews, 13, 318–345 (2009).

[8] B. Frank, *Phase change material for space heating and cooling*, Sustainable Energy Center: University of South Australia (2002).

[9] A. Athienitis and Y. Chen, *The effect of solar radiation on dynamic thermal performance of floor heating systems,* Solar Energy 69, 229-237 (2000).

[10] K.P. Lin, Y.P. Zhang, X. Xu, H.F. Di, R. Yang and P.H. Qin, *Modeling and simulation of under-floor electric heating system with shape-stabilized PCM plates*, Building and Environment 39, 1427-1434 (2004).

[11] K. Nagano, T. Mochida, K. Iwata, H. Hiroyoshi, R. Domanski and M. Rebow, *Development of new PCM for TES of the cooling system*, Terrastock. In: Benner M, Hahne EWP Eds., 8th International Conference on Thermal Energy Storage, pp 345-350 (2000).

[12] Information on http://www.engineersedge.com/properties of metals.htm

[13] David E. Stier, U.S. Patent number: 6286754 (2001).

[14] G.N. Tiwari, in: Solar Energy - *Fundamentals, Model, Modelling and Applications*, Narosa Publishing House, Inida (2002).

[15] N. Ito, K. Kimura and J. Oka: ASHRAE Transactions (1972).

[16) H.P. Garg, in: Treatise on solar energy, *Fundamentals of Solar Energy*, Vol.1, Chapter 3, Chichester: Wiley Publisher (1982).

[17] C. Chen, H.F. Guo, Y.N. Liu, H.L. Yue and C.D. Wang, *A new kind of Phase change material for energy-storing wallboard*, Energy and Buildings, 40 (5), 882-890 (2008).